



Published in final edited form as:

*Biomol NMR Assign.* 2012 April ; 6(1): 95–98. doi:10.1007/s12104-011-9333-2.

## **<sup>1</sup>H, <sup>13</sup>C, and <sup>15</sup>N resonance assignments and secondary structure prediction of the full-length transition state regulator AbrB from *Bacillus anthracis***

**Andrew L. Olson,**

Department of Molecular and Structural Biochemistry, North Carolina State University, Raleigh, NC 27695, USA

**Benjamin G. Bobay,**

Department of Molecular and Structural Biochemistry, North Carolina State University, Raleigh, NC 27695, USA

**Christian Melander,** and

Department of Chemistry, North Carolina State University, Raleigh, NC 27695, USA

**John Cavanagh**

Department of Molecular and Structural Biochemistry, North Carolina State University, Raleigh, NC 27695, USA

### **Abstract**

The AbrB protein is a transcription factor that regulates the expression of numerous essential genes during the cells transition phase state. AbrB from *Bacillus anthracis* is, notoriously, the principal protein responsible for anthrax toxin gene expression and is highly homologous to the much-studied AbrB protein from *Bacillus subtilis* having 85% sequence identity and the ability to regulate the same target promoters. Here we report back-bone and sidechain resonance assignments and secondary structure prediction for the full-length AbrB protein from *B. anthracis*.

### **Keywords**

AbrB; NMR; *Bacillus anthracis*; Transition state regulator

### **Biological context**

Transition state regulator (TSR) proteins are essential for cell survival in hostile and fluctuating environments. They regulate gene expression for countless bacterial responses such as biofilm development, sporulation, toxin secretion, competence, and even complete physiological transformations (Sonenshein et al. 2002; Strauch and Hoch 1993). The transcription factor AbrB is the most widely studied TSR from a genetic and biochemical standpoint and is part of a complex and interconnected regulatory pathway in which AbrB alone has the ability to regulate the expression of more than 60 genes directly and many more due to regulation of other regulatory proteins (Bobay et al. 2004; Chumsakul et al. 2011). AbrB-like TSR's are present in many health-related organisms, in particular, *Bacillus anthracis*, the Gram-positive sporulating bacterium responsible for anthrax toxin secretion. It

has been shown that direct binding of AbrB to the *atxA* promoter is responsible for toxic gene expression in *B. anthracis* (Saile and Koehler 2002; Strauch et al. 2005).

From a structural viewpoint, AbrB from *Bacillus subtilis* is the only TSR to be characterized to any extent is (Bobay et al. 2005; Coles et al. 2005). In these studies, only the N-terminal domain of AbrB was evaluated, and analysis of the full-length protein has remained elusive. Interestingly, examination of dozens of chromosomal AbrB binding sites has failed to identify a consensus sequence that adequately explains AbrB site selection and recognition. It has been suggested that AbrB binding requires a specific three-dimensional conformation of the DNA helix (Bobay et al. 2006; Sullivan et al. 2008). Consequently, structural studies of full-length AbrB are important.

AbrB consists of 94 residues (10.5 kDa) forming a challenging homotetramer of identical subunits (Benson et al. 2002) The monomer consists of two domains with the N-terminal domain forming a looped-hinge helix fold involved in DNA binding and C-terminal multimerization domain (Bobay et al. 2005; Coles et al. 2005; Phillips and Strauch 2001). The homolog from *Bacillus anthracis* is nearly identical to *B. subtilis* with 80 out of 94 residues in the sequence the same and the first 62 residues (N-terminal domain) being identical. It was found that AbrB from both organisms can interchangeably regulate the same target promoters, even those promoters absent from their respective organism processes (Strauch et al. 2005). Their ability to regulate the same promoters and their nearly identical homology indicates very similar structures with only differentiation in the C-terminal multimerization domains. As a first step toward solving the NMR solution structure of full-length AbrB, we report nearly complete sequence specific backbone and sidechain chemical shift assignments of AbrB from *B. anthracis*.

## Methods and experiments

Full length AbrB (residues 1–94) from *B. anthracis* was cloned into expression vector pET-28a (Novagen) with a Thrombin cleavable N-terminal histidine tag and transformed into BL21(DE3) cells (Genesee) for expression. To uniformly label AbrB with  $^{13}\text{C}/^{15}\text{N}$ , cells were grown in 1 L of M9 media supplemented with  $^{15}\text{NH}_4\text{Cl}$  and/or  $^{13}\text{C}$ -glucose at 37°C. At  $\text{OD}_{600}$  of ~0.7 the temperature was reduced to 30°C and expression induced with 1 mM IPTG. The cells were harvested by centrifugation 4 h postinduction at  $7,000 \times g$  for 15 min. Cell pellets were suspended in lysis buffer (10 mM Tris-HCl, 300 mM KCl, 1 mM DTT, 5 mM imidazole, and 0.02% sodium azide) and sonicated with resulting cell lysate clarified by centrifugation at  $15,000 \times g$  and the resulting supernatant was passed over Ni-NTA agarose resin (Qiagen). The N-terminal histidine tag was removed from the purified protein by incubation with Thrombin and loaded onto a Q-Sepharose ion exchange column (GE Healthcare). Samples for NMR experiments were dialyzed into NMR buffer (10 mM  $\text{KH}_2\text{PO}_4$ , 15 mM KCl, 1 mM DTT, 1 mM EDTA, 0.02% sodium azide, in 10 and 100%  $\text{D}_2\text{O}$ ) at pH 6.0 and concentrated to 500–750  $\mu\text{M}$ .

All NMR experiments were performed at 310 K on a Varian Inova 600 MHz and Bruker Avance 700 MHz, both equipped with cryoprobes. Backbone chemical shifts were assigned in a sequential manner from the following experiments: 2D [ $^{15}\text{N}$ - $^1\text{H}$ ] TROSY-HSQC, HNC0, HN(CA)CO, CBCA(CO)NH, HNCACB, and a CC(CO)NH.

Sidechain proton chemical shifts were assigned using the following experiments: HBHA(CO)NH, (H)CC(CO)NH,  $^{15}\text{N}$ -TOCSY (50 and 100 ms), and an HCCH-TOCSY. Aromatic assignments were made from a  $^{13}\text{C}$ -aromatic NOESY (100 ms). Data was processed using NMRPipe (Delaglio et al. 1995) and analyzed using Sparky (Goddard and Kneller 2006) and NMRView (Johnson and Blevins 1994). Phi/Psi dihedral angles and

resulting secondary structure prediction was calculated using the program PREDITOR and protein flexibility was estimated using the Random Coil Index (RCI) (Berjanskii et al. 2006; Berjanskii and Wishart 2007).

## Assignments and data deposition

Complete backbone amide assignments have been obtained for all non-proline residues 2–94 as shown in the 2D [ $^1\text{H}$ - $^{15}\text{N}$ ] TROSY-HSQC spectrum in Fig. 1. Near complete backbone resonances for C $\alpha$  (98%), C $\beta$  (99%), C' (98%), Ha (100%) have been assigned including 96% of sidechain and 100% of aromatic proton resonances. The N-terminal (2–53) chemical shifts of the full length AbrB from *B. anthracis* (Fig. 1) are nearly the same to the those [ $^1\text{H}$ - $^{15}\text{N}$ ]-HSQC chemical shifts reported for the N-terminal domain of AbrB from *B. subtilis* indicating that these domains are identical (Bobay et al. 2005).

Chemical shift index using PREDITOR in Fig. 2a indicates a very well structured N-terminal domain (residues 2–53) with a  $\beta\beta\alpha\beta\beta$  secondary structure-folding pattern identical to that of the published N-terminal AbrB structure from *B. subtilis* (Bobay et al. 2005, Coles et al. 2005). The secondary structure prediction for the C-terminal domain (residues 54–94) in Fig. 2 shows two long helices from residues 55–70 and 74–90. These two helices most likely multimerize with the C-terminus of an adjacent AbrB molecule, likely forming a bundle of four helices in forming the homotetramer. A modest increase in the Random Coil Index (Fig. 2b) in the C-terminal residues (when compared to N-terminal structured regions) indicates a rather dynamic multimerization interaction between C-terminal domains potentially necessary for AbrB's promiscuous DNA binding (Sullivan et al. 2008). The chemical shift assignments have been deposited in the BioMagResBank (<http://www.bmrb.wisc.edu>) under the accession number 17650.

## Acknowledgments

This work is supported by a NIH grant (GM55769) and Department of Defense grant (DM090298) to JC and CM.

## References

- Benson LM, Vaughn JL, Strauch MA, Bobay BG, Thompson R, Naylor S, et al. Macromolecular assembly of the transition state regulator AbrB in its unbound and complexed states probed by microelectrospray ionization mass spectrometry. *Anal Biochem.* 2002; 306(2):222–227. [PubMed: 12123659]
- Berjanskii MV, Wishart DS. The RCI server: rapid and accurate calculation of protein flexibility using chemical shifts. *Nucleic Acids Res.* 2007; 35(2):W531–W537. [PubMed: 17485469]
- Berjanskii MV, Neal S, Wishart DS. PREDITOR: a web server for predicting protein torsion angle restraints. *Nucleic Acids Res.* 2006; 34(2):W63–W69. [PubMed: 16845087]
- Bobay BG, Benson L, Naylor S, Feeney B, Clark AC, Goshe MB, et al. Evaluation of the DNA binding tendencies of the transition state regulator AbrB. *Biochem (NY).* 2004; 43(51):16106–16118.
- Bobay BG, Andreeva A, Mueller GA, Cavanagh J, Murzin AG. Revised structure of the AbrB N-terminal domain unifies a diverse superfamily of putative DNA-binding proteins. *FEBS Lett.* 2005; 579(25):5669–5674. [PubMed: 16223496]
- Bobay BG, Mueller GA, Thompson RJ, Murzin AG, Venters RA, Strauch MA, et al. NMR structure of AbhN and comparison with AbrBN: first insights into the DNA binding promiscuity and specificity of AbrB-like transition state regulator proteins. *J Biol Chem.* 2006; 281:21399–21409. [PubMed: 16702211]
- Chumsakul O, Takahashi H, Oshima T, Hishimoto T, Kanaya S, Ogasawara N, et al. Genome-wide binding profiles of the *Bacillus subtilis* transition state regulator AbrB and its homolog Abh reveals

their interactive role in transcriptional regulation. *Nucleic Acids Res.* 2011; 39(2):414–428. [PubMed: 20817675]

- Coles M, Djuranovic S, Söding J, Frickey T, Koretke K, Truffault V, et al. AbrB-like transcription factors assume a swapped hairpin fold that is evolutionarily related to double-psi  $\beta$  barrels. *Structure.* 2005; 13(6):919–928. [PubMed: 15939023]
- Delaglio F, Grzesiek S, Vuister GW, Zhu G, Pfeifer J, Bax A. NMRPipe: a multidimensional spectral processing system based on UNIX pipes. *J Biomol NMR.* 1995; 6(3):277–293. [PubMed: 8520220]
- Goddard, TD.; Kneller, DG. Sparky 3. University of California; San Francisco: 2006.
- Johnson BA, Blevins RA. NMR view: a computer program for the visualization and analysis of NMR data. *J Biomol NMR.* 1994; 4(5):603–614. [PubMed: 22911360]
- Phillips ZEV, Strauch MA. Role of Cys54 in AbrB multimerization and DNA-binding activity. *FEMS Microbiol Lett.* 2001; 203(2):207–210. [PubMed: 11583849]
- Saile E, Koehler TM. Control of anthrax toxin gene expression by the transition state regulator AbrB. *J Bacteriol.* 2002; 184:370–380. [PubMed: 11751813]
- Sonenshein, AL.; Hoch, JA.; Losick, R. *Bacillus subtilis* and its closest relatives: from genes to cells. ASM Press; Washington DC: 2002.
- Strauch MA, Hoch JA. Transition-state regulators: sentinels of *Bacillus subtilis* post-exponential gene expression. *Mol Microbiol.* 1993; 7(3):337–342. [PubMed: 8459762]
- Strauch MA, Ballar P, Rowshan AJ, Zoller KL. The DNA-binding specificity of the *Bacillus anthracis* AbrB protein. *Microbiology.* 2005; 151(6):1751–1759. [PubMed: 15941984]
- Sullivan DM, Bobay BG, Kojetin DJ, Thompson RJ, Rance M, Strauch MA, et al. Insights into the nature of DNA binding of AbrB-like transcription factors. *Structure.* 2008; 16(11):1702–1713. [PubMed: 19000822]

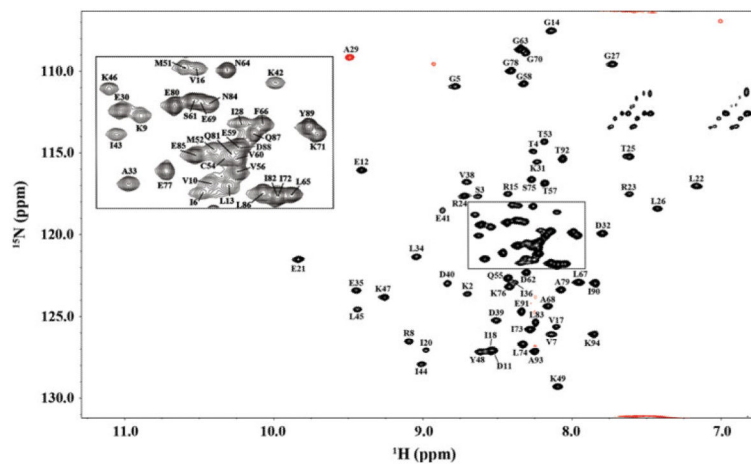


**Fig. 1.** 2D [ $^1\text{H}$ - $^{15}\text{N}$ ] TROSY-HSQC spectrum of 750  $\mu\text{M}$  AbrB protein from *Bacillus anthracis* in 10 mM KCl, 15 mM  $\text{KH}_2\text{PO}_4$ , 1 mM EDTA, 1 mM DTT, and 0.02% sodium azide at 700 MHz spectrometer. Note that residue A29 is folded from 133 ppm

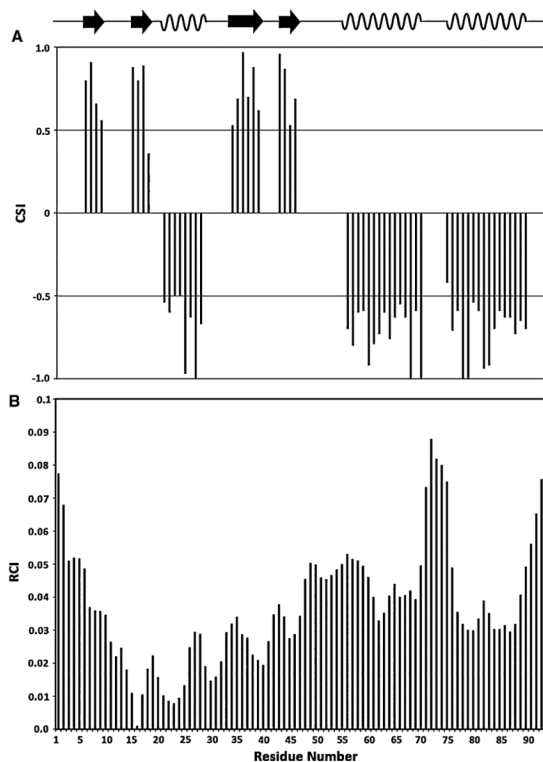


**Fig. 2.**  
**a** Chemical shift index as determined from PREDITOR using backbone  $C\alpha$ ,  $C\beta$ ,  $H\alpha$ , and  $C'$  atoms. Bar magnitudes indicate relative confidence in prediction with areas of *positive values* indicating extended sheet regions and *negative values* indicating helical secondary structure. **b** Random coil index indicating protein flexibility corresponding to secondary structure predicted from CSI